

DCT-Based General Structure for Linear-Phase Paraunitary Filterbanks

Jie Liang, *Student Member, IEEE*, Trac D. Tran, *Member, IEEE*, and Ricardo L. de Queiroz, *Senior Member, IEEE*

Abstract—In this paper, we present a general structure for linear phase paraunitary filterbanks (LPPUFB) via both time-domain pre-processing and frequency-domain post-processing of the discrete cosine transform (DCT). The proposed structure not only covers existing frameworks with either pre-processing or post-processing of the DCT but enables the design of DCT-based LPPUFB with both partial-block overlapping and variable-length filters as well. Some high-performance and low-complexity transforms can be obtained by fine-tuning the structure parameters. Furthermore, a DCT-oriented initialization method is developed to improve the convergence and to simplify the parameterization in the filterbank optimization process. The application in image compression is demonstrated.

Index Terms—DCT, lapped transform, linear-phase paraunitary filterbank, pre-processing, post-processing.

I. INTRODUCTION

THE Type-II discrete cosine transform (DCT-II) [1] has found wide applications in image and video compression, due to its excellent energy compaction capability and to the existence of numerous fast implementations. However, DCT-based coding schemes exhibit annoying blocking artifacts at low bit rates. The lapped orthogonal transform (LOT) [2], [3] provides a solution to this problem via post-processing of the DCT coefficients. The basis functions of the LOT cover two data blocks. Further suppression of blocking artifacts can be achieved by employing multistage post-processing, as in the generalized LOT (GenLOT) [4].

The GenLOT is developed on the framework of linear-phase paraunitary filterbanks (LPPUFB) [5], [6]. In [7], the complete and minimal factorization of even-channel LPPUFB via the lattice structure is developed. The structure is generalized to cover a large class of perfect reconstruction filterbanks in [8]. Recently, it was shown in [9] and [10] that the structures in [7] and [8] can be simplified significantly and still cover the same solution sets. Since the DCT, LOT, and GenLOT are all special cases of LPPUFB, the theory of LPPUFB is very powerful in the design and analysis of such transforms. In fact, the LOT in [2] is an elegant fast approximation of the optimal M -channel, $2M$ -tap LPPUFB.

Manuscript received February 21, 2002; revised December 6, 2002. This work was supported by the National Science Foundation under CAREER Grant CCR-0093262. The associate editor coordinating the review of this paper and approving it for publication was Dr. Xiang-Gen Xia.

J. Liang and T. D. Tran are with the Department of Electrical and Computer Engineering, The Johns Hopkins University, Baltimore, MD 21218 USA (e-mail: jliang@jhu.edu; trac@jhu.edu).

R. L. de Queiroz is with Corporate Research and Technology, the Xerox Corporation, Webster, NY, 14580 USA (e-mail: queiroz@ieee.org).

Digital Object Identifier 10.1109/TSP.2003.811224

In addition to post-processing of the DCT coefficients, various transforms involving pre-processing of the DCT inputs have also been proposed. However, most existing results focus on the modulation of DCT-III or DCT-IV [1] and are therefore not suitable for image representation. For example, the widely used modulated lapped transform (MLT) and extended lapped transform (ELT) [2] in audio compression are based on the DCT-IV. In [11], the MLT/ELT idea is generalized to implement arbitrary-length cosine-modulated filterbanks [12], [13] through pre-processing of the DCT-III or the DCT-IV.

An early effort of improving the performance of image compression through pre-processing of the DCT-II can be found in [14]. Recently, a more general family called the time-domain lapped transform (TDLT) was developed in [15].

Pre-processing or post-processing of the DCT generates transforms with different properties. In the LOT/GenLOT case, by varying the sizes of post-processing stages, different subbands can have basis functions of different lengths [16]–[18]. This enables the transform to have longer filters for low-frequency subbands and shorter filters for high-frequency subbands, maintaining a balance between reducing blocking artifacts and avoiding ringing artifacts. Analogously, reducing the size of the pre-processing operator in the TDLT leads to transforms with partial-block overlapping, which can also be exploited to obtain a tradeoff between complexity and performance [15].

In this paper, we show that the DCT can be embedded in any stage of the LPPUFB lattice, resulting in a general structure that involves both multistage time-domain pre-processing and multistage frequency-domain post-processing of the DCT. We call this structure the time–frequency lapped orthogonal transform (TFLOT).

All aforementioned DCT-based structures can be viewed as special cases of our proposed scheme. Moreover, the presence of the DCT in the general structure ensures the robustness of the transform optimization process. In fact, we derive an initialization method for pre- and post-processing operators, allowing the optimization process to start with a reasonable solution. The method also helps in simplifying the parameterization involved.

The intuition behind the proposed structure is as follows. The pre-processing stages manipulate the input data such that they are more suitable for the DCT decomposition. The number of pre-processing stages and their sizes determine the amount of samples being examined in the DCT stage. The post-processing stages are used to further reduce the correlation after the DCT. This suggests that given the length of the filterbank, we can choose the numbers of pre-processing stages and post-processing stages in different ways to take full advantage of them.

The flexibility provided by the proposed structure is very useful in the design of fast transforms. Since the correlation in real-life signals such as images and video sequences weakens gradually as we move away from the current coding block, a few number of pre-processing stages is usually sufficient to get a near-optimal performance. However, when the number of pre-processing stages is limited by complexity constraints, more long-term low-frequency correlation exists after the DCT. This can be clearly observed if all DC coefficients are collected together. With our proposed structure, we can improve the performance by applying post-processing operators. The advantages are twofold. First, the presence of the post-processing makes it possible to further reduce the complexity of the pre-processing without sacrificing the performance. Second, since most high-frequency correlation has been removed by the pre-processing and the DCT, we only need to apply post-processing operators to the low-frequency subbands. Therefore, high-performance and low-complexity transforms can be obtained by the joint design of the pre- and post-processing. The different properties of the pre- and post-processing operators can be exploited to obtain transforms with both variable-length filters and partial-block overlapping without modifying the DCT. Our intuition is later confirmed in the design and coding experiments.

II. GENERAL STRUCTURE OF DCT-BASED LPPUFB

In this section, we consider a real-coefficient M -channel, KM -tap (M even, K integer) linear-phase paraunitary filterbank, or an $M \times KM$ LPPUFB for short. All filters are either symmetric or anti-symmetric, i.e., the polyphase matrix $\mathbf{E}(z)$ satisfies

$$\mathbf{D}z^{(K-1)}\mathbf{E}(z^{-1})\mathbf{J} = \mathbf{E}(z) \quad (1)$$

where \mathbf{J} is the reversal identity matrix, and \mathbf{D} is a diagonal matrix whose diagonal entries are ± 1 's, with $+1$'s correspond to symmetric filters and -1 's correspond to anti-symmetric ones.

A. Existing Structure

The general structure of LPPUFB is developed in [7], by which $\mathbf{E}(z)$ can be factorized as

$$\mathbf{E}(z) = \mathbf{G}_{K-1}(z)\mathbf{G}_{K-2}(z)\dots\mathbf{G}_1(z)\mathbf{E}_0 \quad (2)$$

where

$$\mathbf{E}_0 = \text{diag}\{\mathbf{U}_0, \mathbf{V}_0\}\hat{\mathbf{W}} \quad (3)$$

$$\Lambda(z) = \text{diag}\{z\mathbf{I}, \mathbf{I}\} \quad (4)$$

$$\mathbf{G}_i(z) = \text{diag}\{\mathbf{U}_i, \mathbf{V}_i\}\mathbf{W}\Lambda(z)\mathbf{W}. \quad (5)$$

\mathbf{W} and $\hat{\mathbf{W}}$ in the above are two kinds of butterfly given by

$$\mathbf{W} = \frac{1}{\sqrt{2}} \begin{bmatrix} \mathbf{I} & \mathbf{I} \\ \mathbf{I} & -\mathbf{I} \end{bmatrix}, \quad \hat{\mathbf{W}} = \frac{1}{\sqrt{2}} \begin{bmatrix} \mathbf{I} & \mathbf{J} \\ \mathbf{J} & -\mathbf{I} \end{bmatrix} \quad (6)$$

where \mathbf{I} and \mathbf{J} are $M/2 \times M/2$ identity and reversal matrix, respectively.

The matrices \mathbf{U}_i and \mathbf{V}_i in (3) and (5) are arbitrary $M/2 \times M/2$ orthogonal matrices. They can be optimized for the objec-

tive function of interests. Recently, it has been shown in [9] and [10] that all \mathbf{U}_i or all \mathbf{V}_i in $\mathbf{G}_i(z)$ can be eliminated, and the completeness of the structure is still guaranteed by having both \mathbf{U}_0 and \mathbf{V}_0 in \mathbf{E}_0 . Therefore, $\mathbf{G}_i(z)$ can be reduced to

$$\mathbf{G}_i(z) = \text{diag}\{\mathbf{I}, \mathbf{V}_i\}\mathbf{W}\Lambda(z)\mathbf{W}. \quad (7)$$

The complexity of the structure is thus reduced significantly.

B. DCT-Based Structure

We now show that the DCT can be embedded in \mathbf{E}_0 or any stage $\mathbf{G}_i(z)$ of the general structure without affecting its completeness. In addition to fast implementation, the presence of the DCT can also be exploited in the filterbank optimization, as illustrated in Section III.

Recall that the Type-II DCT can be factorized as

$$\mathbf{C} = \text{diag}\{\mathbf{C}_0, \mathbf{C}_1\}\hat{\mathbf{W}} \quad (8)$$

where \mathbf{C}_0 and \mathbf{C}_1 are $M/2$ -point Type-II and Type-IV DCT, respectively [1].

As a first step, notice that by taking advantage of the property that $\text{diag}\{\mathbf{U}_0, \mathbf{U}_0\}$ commutes with \mathbf{W} and $\Lambda(z)$ [10], \mathbf{U}_0 in \mathbf{E}_0 can actually be located in any stage $\mathbf{G}_N(z)$ ($1 \leq N \leq K-1$) rather than \mathbf{E}_0 . That is, we can have an equivalent structure to that in [9] and [10] by defining

$$\begin{aligned} \mathbf{E}_0 &= \text{diag}\{\mathbf{I}, \mathbf{V}_0\}\hat{\mathbf{W}} \\ \mathbf{G}_N(z) &= \text{diag}\{\mathbf{U}_0, \mathbf{V}_N\}\mathbf{W}\Lambda(z)\mathbf{W}. \end{aligned} \quad (9)$$

The remaining stages $\mathbf{G}_i(z)$ still follow (7).

To get a modular structure, we can turn all \mathbf{W} in $\mathbf{G}_i(z)$ into $\hat{\mathbf{W}}$ for $i = 1, \dots, N$ by the following relationship between the two types of butterfly

$$\hat{\mathbf{W}} = \text{diag}\{\mathbf{I}, \mathbf{J}\}\mathbf{W}\text{diag}\{\mathbf{I}, \mathbf{J}\}. \quad (10)$$

This also changes the corresponding \mathbf{V}_i 's to $\mathbf{V}'_0 = \mathbf{J}\mathbf{V}_0$, $\mathbf{V}'_N = \mathbf{V}_N\mathbf{J}$, and $\mathbf{V}'_i = \mathbf{J}\mathbf{V}_i\mathbf{J}$ for $i = 1, \dots, N-1$. After simple regrouping, we arrive at

$$\mathbf{G}_N(z)\dots\mathbf{G}_1(z)\mathbf{E}_0 = \hat{\mathbf{E}}_0\mathbf{P}_{N-1}(z)\dots\mathbf{P}_0(z) \quad (11)$$

where

$$\hat{\mathbf{E}}_0 = \text{diag}\{\mathbf{U}_0, \mathbf{V}'_N\}\hat{\mathbf{W}} \quad (12)$$

and $\mathbf{P}_i(z)$ ($i = 0, \dots, N-1$) is defined by

$$\mathbf{P}_i(z) = \Lambda(z)\hat{\mathbf{W}}\text{diag}\{\mathbf{I}, \mathbf{V}'_i\}\hat{\mathbf{W}}. \quad (13)$$

Now, we can introduce the DCT into $\hat{\mathbf{E}}_0$ by

$$\begin{aligned} \hat{\mathbf{E}}_0 &= \text{diag}\{\mathbf{U}_0\mathbf{C}_0^T, \mathbf{V}'_N\mathbf{C}_1^T\}\text{diag}\{\mathbf{C}_0, \mathbf{C}_1\}\hat{\mathbf{W}} \\ &= \text{diag}\{\mathbf{U}'_0, \mathbf{V}''_N\}\mathbf{C} \end{aligned} \quad (14)$$

where \mathbf{C} , \mathbf{C}_0 , and \mathbf{C}_1 are defined in (8).

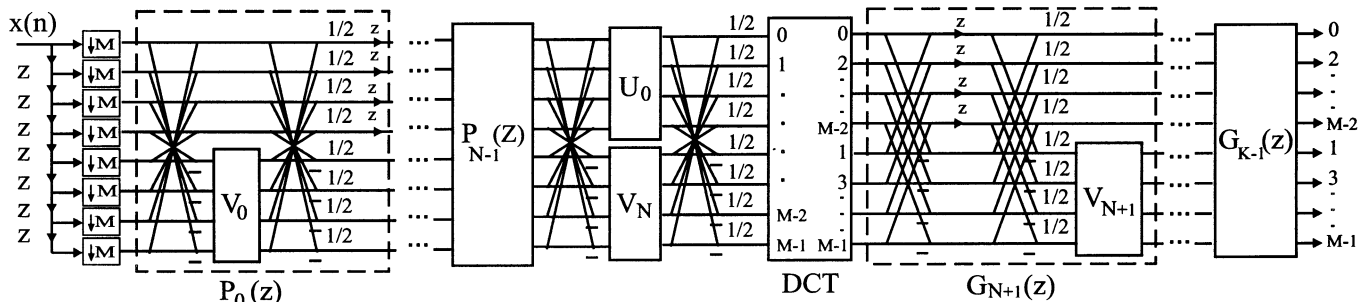


Fig. 1. General structure of the TFLOT.

Alternatively, the DCT can be embedded through

$$\begin{aligned} \hat{\mathbf{E}}_0 &= \mathbf{C}\mathbf{C}^T \hat{\mathbf{E}}_0 \\ &= \mathbf{C}\hat{\mathbf{W}}\text{diag}\{\mathbf{C}_0^T \mathbf{U}_0, \mathbf{C}_1^T \mathbf{V}'_N\} \hat{\mathbf{W}} \\ &= \mathbf{C}\hat{\mathbf{W}}\text{diag}\{\mathbf{U}'_0, \mathbf{V}''_N\} \hat{\mathbf{W}}. \end{aligned} \quad (15)$$

If the objective is to embed the DCT in \mathbf{E}_0 , the step of moving \mathbf{U}_0 into $\mathbf{G}_N(z)$ and the subsequent regrouping are not needed. We only need to start from (14) or (15).

The above manipulations to obtain \mathbf{U}'_0 , \mathbf{V}''_N , and \mathbf{V}'_i 's impose no constraint on them; therefore, each of them can still be modeled by a generic orthogonal matrix. To summarize, we obtain the following result.

Corollary 1: The polyphase matrix $\mathbf{E}(z)$ of any $M \times KM$ LPPUFB can be factorized as

$$\mathbf{E}(z) = \mathbf{G}_{K-1}(z) \dots \mathbf{G}_{N+1}(z) \hat{\mathbf{E}}_0 \mathbf{P}_{N-1}(z) \dots \mathbf{P}_0(z) \quad (16)$$

where the DCT-based $\hat{\mathbf{E}}_0$ can take the form in (14) or (15), and $\mathbf{G}_i(z)$ and $\mathbf{P}_i(z)$ are given in (7) and (13), respectively.

Remarks: This structure is depicted in Fig. 1 when (15) is used. Since it involves both time-domain pre-processing and frequency-domain post-processing of the DCT, we denote it as the TFLOT. Because of the presence of the DCT in the TFLOT, the fast implementation of the DCT can be applied. In addition, since the DCT already has good energy compaction capability, it can be exploited in the filterbank optimization, as reported in Section III.

All existing DCT-based structures for LPPUFB can be viewed as special cases of the TFLOT. For example, if we embed the DCT in \mathbf{E}_0 , the TFLOT reduces to the GenLOT [4]. Especially, when the filter length is $2M$, the general structure can be simplified to the LOT in [2]. On the other hand, if we insert the DCT in $\mathbf{G}_{K-1}(z)$, the structure can be viewed as multistage time-domain pre-processing of the DCT input. It can be viewed as the dual of the GenLOT and the generalization of the fast TDLT in [15]. We denote this special case as the GenTDLT.

In the TFLOT, variable-length filters can be obtained by limiting the sizes of the last several post-processing stages [16]–[18], whereas partial-block overlapping can be achieved if the size of the first pre-processing stage is reduced [15]. Therefore, when the DCT is embedded in an intermediate stage, variable-length filters and partial-block overlapping can be maintained simultaneously without modifying the M -point

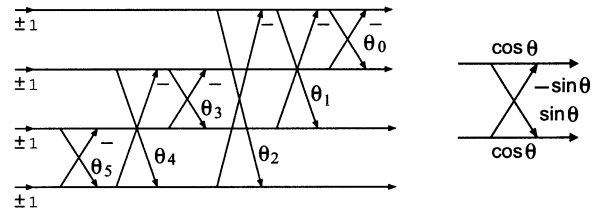


Fig. 2. Left: Example of representing a real orthogonal matrix by Givens rotations and signs. Right: Detail of a Givens rotation.

DCT. That is, the TFLOT is able to combine the advantages of both pre-processing and post-processing. High-performance and low-complexity solutions can be obtained in this way, as illustrated in Section IV.

III. DCT-BASED OPTIMIZATION OF THE TFLOT

Unconstrained optimization is a common tool for the design of filterbanks [4]–[6], [9]. Each $M/2 \times M/2$ orthogonal matrix in the lattice structure can be parameterized by $\binom{M/2}{2}$ Givens plane rotations and $M/2$ sign parameters, as illustrated by the example in Fig. 2 [5]. Since most optimization techniques are not efficient in handling continuous and discrete parameters jointly, a common approach is to fix the sign parameters during optimization. However, a thorough analysis must be conducted to make sure that the reduced search space still covers the optimal result.

The most widely used optimization criteria for filterbank design include coding gain, DC attenuation, mirror frequency attenuation, and stopband attenuation. In many cases, the objective function is a weighted combination of them. These criteria are highly nonconvex; hence, the quality of the initialization is crucial to the final result.

Since the DCT has good energy compaction capability, it is a close neighbor of the optimal solution in the search space. Therefore, in the optimization of the TFLOT, we can choose the initial values of all free matrices such that the optimization process always starts from the DCT. In addition to the improved convergence, this initialization method can also help to determine the sign parameters in modeling orthogonal matrices.

A. DCT-Oriented Initialization

In this section, we consider the TFLOT when $\hat{\mathbf{E}}_0$ is chosen as (15) and suppose that the DCT is in stage N . To get the DCT-oriented initialization, we want to initialize the free matrices such that all pre- and post-processing stages are annihilated.

1) *Initialization of the Pre-Processing Stages:* We first develop the DCT-oriented initialization for the pre-processing stages of the DCT. Define

$$\mathbf{E}_N(z) \triangleq \hat{\mathbf{E}}_0 \mathbf{P}_{N-1}(z) \dots \mathbf{P}_0(z). \quad (17)$$

Notice that when $\mathbf{V}_i = -\mathbf{I}$, the pre-processing stage $\mathbf{P}_i(z)$ in (13) becomes

$$\mathbf{P}_i(z) = \begin{bmatrix} \mathbf{0} & z\mathbf{J} \\ \mathbf{J} & \mathbf{0} \end{bmatrix}. \quad (18)$$

The cascade of two such stages gives rise to

$$\mathbf{P}_{i+1}(z)\mathbf{P}_i(z) = \begin{bmatrix} \mathbf{0} & z\mathbf{J} \\ \mathbf{J} & \mathbf{0} \end{bmatrix} \begin{bmatrix} \mathbf{0} & z\mathbf{J} \\ \mathbf{J} & \mathbf{0} \end{bmatrix} = z\mathbf{I}. \quad (19)$$

Therefore, when N is even, by choosing

$$\begin{aligned} \mathbf{U}_0 &= \mathbf{I}, & \mathbf{V}_N &= -\mathbf{I}, \\ \mathbf{V}_0 &= \mathbf{I}, & \mathbf{V}_i &= -\mathbf{I}, \quad i = 1, \dots, N-1 \end{aligned} \quad (20)$$

we have

$$\mathbf{E}_N(z) = \mathbf{C} \begin{bmatrix} \mathbf{0} & \mathbf{J} \\ \mathbf{J} & \mathbf{0} \end{bmatrix} z^{N/2-1} \begin{bmatrix} \mathbf{0} & z\mathbf{J} \\ \mathbf{J} & \mathbf{0} \end{bmatrix} \begin{bmatrix} z\mathbf{I} & \mathbf{0} \\ \mathbf{0} & \mathbf{I} \end{bmatrix} = z^{N/2} \mathbf{C}. \quad (21)$$

This corresponds to a zero-padded DCT with $MN/2$ zeros at each side.

When N is odd, we can choose

$$\begin{aligned} \mathbf{U}_0 &= \mathbf{J}, & \mathbf{V}_N &= -\mathbf{J}, & \mathbf{V}_0 &= \mathbf{I} \\ \mathbf{V}_i &= -\mathbf{I}, & i &= 1, \dots, N-1. \end{aligned} \quad (22)$$

In this case, $\hat{\mathbf{E}}_0$ in (15) reduces to

$$\hat{\mathbf{E}}_0 = \mathbf{C} \begin{bmatrix} \mathbf{0} & \mathbf{I} \\ \mathbf{I} & \mathbf{0} \end{bmatrix} \quad (23)$$

and therefore

$$\mathbf{E}_N(z) = \hat{\mathbf{E}}_0 z^{N-1/2} \begin{bmatrix} z\mathbf{I} & \mathbf{0} \\ \mathbf{0} & \mathbf{I} \end{bmatrix} = z^{\frac{N-1}{2}} \mathbf{C} \begin{bmatrix} \mathbf{0} & \mathbf{I} \\ z\mathbf{I} & \mathbf{0} \end{bmatrix}. \quad (24)$$

The term $\begin{bmatrix} \mathbf{0} & \mathbf{I} \\ z\mathbf{I} & \mathbf{0} \end{bmatrix}$ simply pads $M/2$ zeros to each side of the filterbank. Therefore we also end up with a zero-padded DCT.

When the optimized parameters of a filterbank with $N-1$ pre-processing stages are available, they can be used to initialize the optimization of FB with N pre-processing stages. It can be verified that with

$$\begin{aligned} \mathbf{U}_0 &= \mathbf{U}'_0 \mathbf{J}, & \mathbf{V}_N &= \mathbf{V}'_{N-1} \mathbf{J}, & \mathbf{V}_0 &= \mathbf{I}, & \mathbf{V}_1 &= -\mathbf{J} \mathbf{V}'_0 \mathbf{J} \\ \mathbf{V}_i &= \mathbf{J} \mathbf{V}'_{i-1} \mathbf{J}, & i &= 2, \dots, N-1 \end{aligned} \quad (25)$$

the following zero-padded result can be obtained:

$$\mathbf{E}_N(z) = \mathbf{E}'_{N-1}(z) \begin{bmatrix} \mathbf{0} & \mathbf{I} \\ z\mathbf{I} & \mathbf{0} \end{bmatrix}. \quad (26)$$

In (25), $\mathbf{U}_0, \mathbf{V}_i$ are matrices for the filterbank with N stages pre-processing, and $\mathbf{U}'_0, \mathbf{V}'_i$ are the given matrices of the filterbank with $N-1$ stages of pre-processing.

2) *Initialization of the Post-Processing Stages:* Suppose the DCT-oriented initialization has been applied to the pre-processing stages and (21) or (24) has been obtained. When $\mathbf{V}_i = -\mathbf{I}$ for all post-processing stages, the cascade of two stages becomes $\mathbf{G}_{i+1}(z)\mathbf{G}_i(z) = z\mathbf{I}$. Therefore, the filterbank reduces to

$$\mathbf{E}(z) = \begin{cases} z^n \mathbf{E}_N(z), & \text{if } K - N - 1 = 2n \\ z^n \mathbf{W}(z) \mathbf{E}_N(z), & \text{if } K - N - 1 = 2n + 1 \end{cases} \quad (27)$$

where $\mathbf{W}(z) = \text{diag}\{\mathbf{I}, -\mathbf{I}\} \mathbf{W} \Lambda(z) \mathbf{W}$. This means that when there is an even number of post-processing stages, the result is still a zero-padded DCT after setting all $\mathbf{V}_i = -\mathbf{I}$. When the number of post-processing stages is odd, the result is the DCT followed by two stages of butterflies, which is actually a simple LOT [2]; hence, it can be used as a good initial value for the optimization.

Given an $M \times KM$ filterbank with polyphase matrix $\mathbf{E}(z)$, all matrices in it can be copied directly to initialize a filterbank with one more stage of post-processing. The additional matrix \mathbf{V}_K can be set to $-\mathbf{I}$ (or \mathbf{I}), and we thus get $\mathbf{W}(z)\mathbf{E}(z)$, which yields a good initial value.

B. Determining the Sign Parameters in Matrix Model

As mentioned earlier, one issue in optimization is how to deal with the sign parameters in modeling orthogonal matrices. The DCT-oriented initialization provides important insight about the optimal sign parameters. Since the DCT is quite close to the optimal solution, it is reasonable to assume that each optimal matrix in the lattice structure has the same sign parameters as its DCT-oriented initial value. Therefore, we can fix the sign parameters according to these initial matrices. More generally, each of \mathbf{U}_0 and \mathbf{V}_i can be modeled as

$$\mathbf{X} = \hat{\mathbf{X}} \mathbf{X}_0 \quad (28)$$

where \mathbf{X}_0 is fixed as the DCT-oriented initial matrix, containing the sign parameters implicitly, and $\hat{\mathbf{X}}$ is the free matrix for the optimization program, whose signs can be safely fixed as $+1$'s. The initial value of $\hat{\mathbf{X}}$ is simply \mathbf{I} and can be obtained by setting all Givens rotation angles to be $2n\pi$ (n integer).

Experimental results show that this type of initialization and sign model always lead to satisfactory results. However, different initial angles still have slightly different qualities; thus, we can perform the optimization with different values of n and select the best results among them.

C. Fast Approximations

One important design criterion for image compression is the coding gain. For paraunitary filterbanks, the coding gain is computed as [5], [6]

$$\gamma = 10 \log_{10} \frac{\sigma_x^2}{\left(\prod_{k=0}^{M-1} \sigma_{y_k}^2 \right)^{1/M}} \quad (29)$$

where σ_x^2 is the input variance, and $\sigma_{y_i}^2$ is the variance of the i th subband output. In this paper, the input is assumed to be an AR(1) process with intersample correlation coefficient $\rho = 0.95$, which is a good model for natural images.

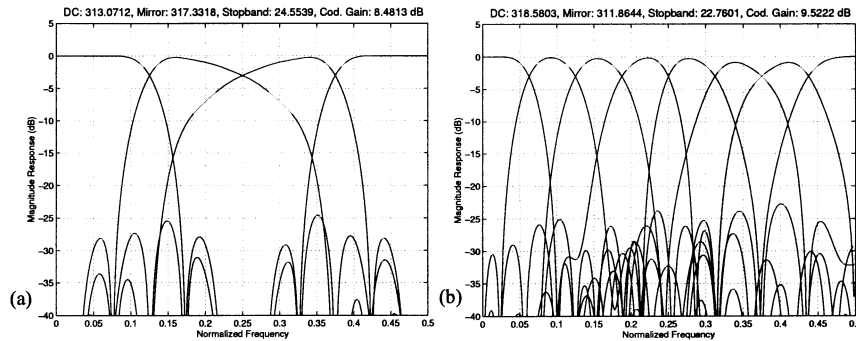


Fig. 3. Frequency response of design examples with fixed \mathbf{U}_0 . The filterbank size is (a) 4×32 and (b) 8×40 .

TABLE I
CODING GAIN IN dB OF EVEN-CHANNEL LPPUFB FOR AN AR(1) SIGNAL WITH $\rho = 0.95$

Size	4×8	4×12	4×16	4×20	4×24	4×28	4×32	4×36	4×40
\mathbf{U}_0 free	7.96	8.22	8.36	8.41	8.45	8.45	8.48	8.48	8.50
\mathbf{U}_0 fixed	7.96	8.20	8.35	8.41	8.45	8.45	8.48	8.48	8.50
Size	6×12	6×18	6×24	6×30	6×36	6×42	6×48	6×54	6×60
\mathbf{U}_0 free	8.85	9.02	9.12	9.19	9.20	9.24	9.25	9.27	9.27
\mathbf{U}_0 fixed	8.85	9.00	9.12	9.19	9.20	9.23	9.25	9.27	9.27
Size	8×16	8×24	8×32	8×40	8×48	8×56	10×20	16×32	16×48
\mathbf{U}_0 free	9.27	9.39	9.46	9.52	9.54	9.56	9.50	9.81	9.86
\mathbf{U}_0 fixed	9.27	9.38	9.46	9.52	9.54	9.56	9.50	9.81	9.85

If coding gain is chosen as the objective function, it is observed that the optimized \mathbf{U}_0 is always very close to its DCT-oriented initial value, i.e.,

$$\begin{aligned} \mathbf{U}_0 &\approx \mathbf{I}, & \text{for even } N \\ \mathbf{U}_0 &\approx \mathbf{J}, & \text{for odd } N. \end{aligned} \quad (30)$$

We can thus fix \mathbf{U}_0 as its initial value to reduce the design complexity. Optimization results show that this does not cause any significant performance degradation.

An additional benefit of the above simplifications is that a constant input would only generate nonzero output in the DC subband, i.e., the resulting filterbank automatically guarantees zero DC leakage, which is another desired property for image compression to avoid checkerboard artifacts [6].

Further approximation can be obtained for an $M \times 2M$ LPPUFB. In this case, both \mathbf{U}_0 and \mathbf{V}_1 can be fixed as their initial values. After simple manipulations, the structure can reduce to the LOT in [2] or the TDLT in [15], depending on whether post-processing or pre-processing is used.

D. Design Examples

Various design results are summarized in Table I, including results with fixed \mathbf{U}_0 . The results are consistent to those reported in [4], [9], and [18], showing the validity of the optimization method. Zero DC leakage and mirror frequency attenuation are guaranteed when \mathbf{U}_0 is fixed according to the DCT-oriented initialization, as can be observed by the frequency response examples in Fig. 3. Table I shows that the performance degradation due to the fixed \mathbf{U}_0 is less than 0.01 dB in almost all cases. Moreover, compared with the DCT, Table I suggests that one stage of pre-processing yields the most significant performance

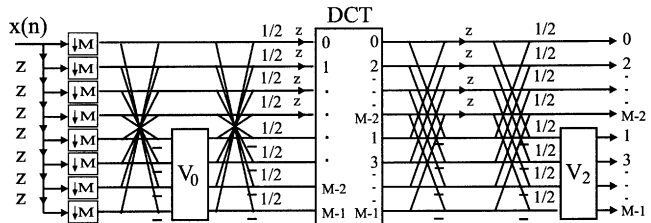


Fig. 4. Fast TFLOT with one pre- and one post-processing stage.

gain for signals with AR(1) model and $\rho = 0.95$. This is also true when pure post-processing is used.

The coding gain of the optimized 8×16 orthogonal TDLT in [15] is 9.26 dB, which is very close to the 9.27 dB of the general structure, showing that the TDLT is an elegant fast approximation of the general $M \times 2M$ LPPUFB.

The TFLOT can be generalized to odd-channel LPPUFB and LPPUFB with pair-wise mirror image (PMI) property. Some design examples can be found in [19].

IV. FAST TFLOT WITH BOTH PRE- AND POST-PROCESSING

In this section, we develop some fast TFLOT examples with both pre- and post-processing of the DCT. To achieve a better tradeoff between the complexity and the performance, we will also design filterbanks with both partial-block overlapping and variable-length filters. Since the DCT is embedded in an intermediate stage, the M -point DCT is intact in the design.

We consider the TFLOT in (16) with $\hat{\mathbf{E}}_0$ given by (14) and $N = 1$, i.e., one pre-processing stage of the DCT, since this is sufficient to get partial-block overlapping. The choice $\mathbf{U}_0 = \mathbf{I}$ is adopted to simplify the structure and guarantee zero DC

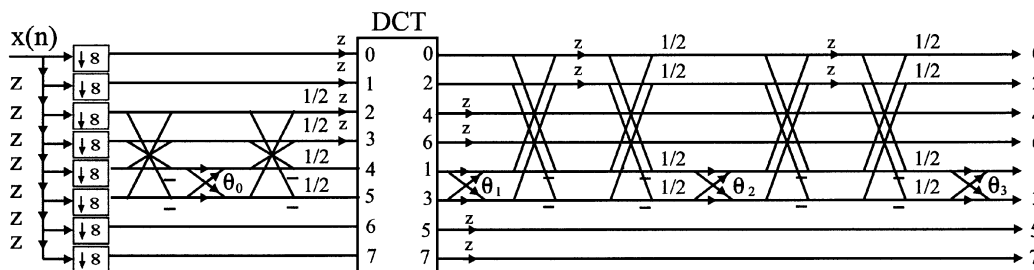


Fig. 5. Fast TFLOT with one pre- and two post-processing stages.

leakage. Further simplifications are also available in different cases. Some examples are presented below.

A. Fast TFLOT With One Post-Processing Stage

When there is only one stage of post-processing, \mathbf{V}_1 can also be fixed as the identity with negligible impact on the performance. The resulting diagram is depicted in Fig. 4, which is an efficient cascade of the TDLT and the LOT. Apart from the DCT, the simplified structure has two $M/2 \times M/2$ matrices. It has lower complexity than the GenLOT and GenTDLT with $\mathbf{U}_0 = \mathbf{I}$.

Fig. 7(a) reports the optimized solution for the 8×24 fast TFLOT according to Fig. 4. Its coding gain is 9.37 dB—very close to the 9.39 dB and 9.38 dB in Table I, corresponding to the cases with free \mathbf{U}_0 and fixed \mathbf{U}_0 , respectively.

This example shows that by distributing the operation into both pre- and post-processing of the DCT, the TFLOT can offer more efficient quasioptimal solution than pure pre-processing or pure post-processing approach.

To further demonstrate the efficiency of the TFLOT in boosting the performance of the DCT, consider Fig. 4 with $M = 8$, and imagine that both \mathbf{V}_0 and \mathbf{V}_2 have the form of $\text{diag}\{\mathbf{V}_i, \mathbf{I}_{(2)}\}$. In this case, each matrix would reduce to a single Givens rotation [5], which can be implemented through three lifting steps, requiring three multiplications and three additions.

The special forms of \mathbf{V}_0 and \mathbf{V}_2 provide small amount of pre- and post-processing to the DCT, leading to a fast TFLOT with both partial-block overlapping and variable-length filters. In fact, it is a 4×20 , 4×12 filterbank, i.e., it has four 20-tap low-frequency basis functions and four 12-tap high-frequency basis functions, as shown in Fig. 7(b). Its optimized coding gain is 9.21 dB, which is between the 9.20 dB of the Type-I fast LOT (LOT-I) and the 9.22 dB of the Type-II fast LOT (LOT-II) in [2].

B. Fast TFLOT With Two Post-Processing Stages

When multiple post-processing stages of the DCT are presented, \mathbf{V}_1 in Fig. 1 cannot be ignored. To reduce the complexity of the transform, consider the fast TFLOT given in Fig. 5, which has one pre-processing stage and two post-processing stages. All effective \mathbf{V}_i 's are taken as 2×2 matrices, and thus, the TFLOT in Fig. 5 is a 4×28 , 4×12 filterbank. Note that an advance unit is introduced to each shorter filter such that all filters have the same center of symmetry, which is desired in image compression [17], [20].

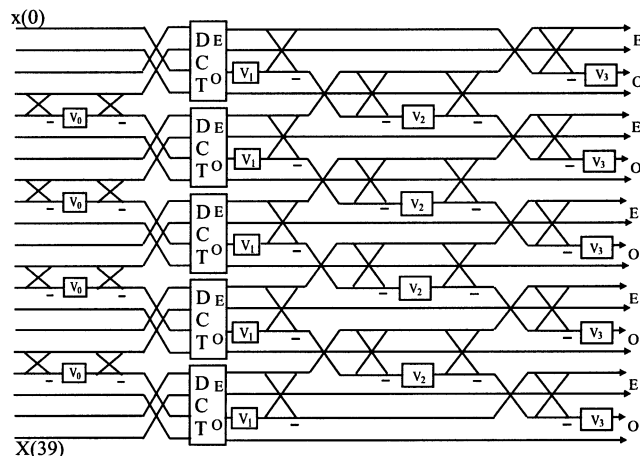


Fig. 6. Implementation example of the fast TFLOT in Fig. 5 for finite-length signals. (Each line carries two samples.)

The implementation of this fast TFLOT for finite-length signals is illustrated in Fig. 6. Recall that the implementation of the LOT requires a boundary processing unit at the DCT stage [2]. This boundary processing is not needed here since we have two post-processing stages. Stage $\mathbf{G}_3(z)$ is aligned with the DCT; therefore, no boundary processing is needed for it. Stages $\mathbf{P}_0(z)$ and $\mathbf{G}_2(z)$ are simply skipped at the boundary. This amounts to applying symmetric extension before $\mathbf{P}_0(z)$ and periodic extension before $\mathbf{G}_2(z)$ such that these stages reduce to the identity, as in [15].

If the pre-processing stage is removed, the filterbank in Fig. 5 becomes a 4×24 , 4×8 filterbank with three rotations. This represents a simplified version of the fast VLOT in [17] with four rotations. The optimized coding gain for this case is 9.27 dB, which is almost identical to the one in [17]. The solution is shown in Fig. 7(c).

When all four rotations are used, the optimized result has a coding gain of 9.33 dB. The corresponding frequency and impulse responses are given in Fig. 7(d). This solution is quite close to the 8×24 fast TFLOT in Fig. 4 but has lower complexity.

Four variable-length GenLOT examples were proposed in [18], requiring four or five stages of post-processing of the DCT, i.e., the filter length is up to 48. The number of rotation angles in them ranges from 6 to 11, and their coding gains are 9.157, 9.287, 9.326, and 9.471 dB, respectively. Compared with them, the TFLOT examples corresponding to Fig. 5 are more cost-effective, due to the combination of pre- and post-processing.

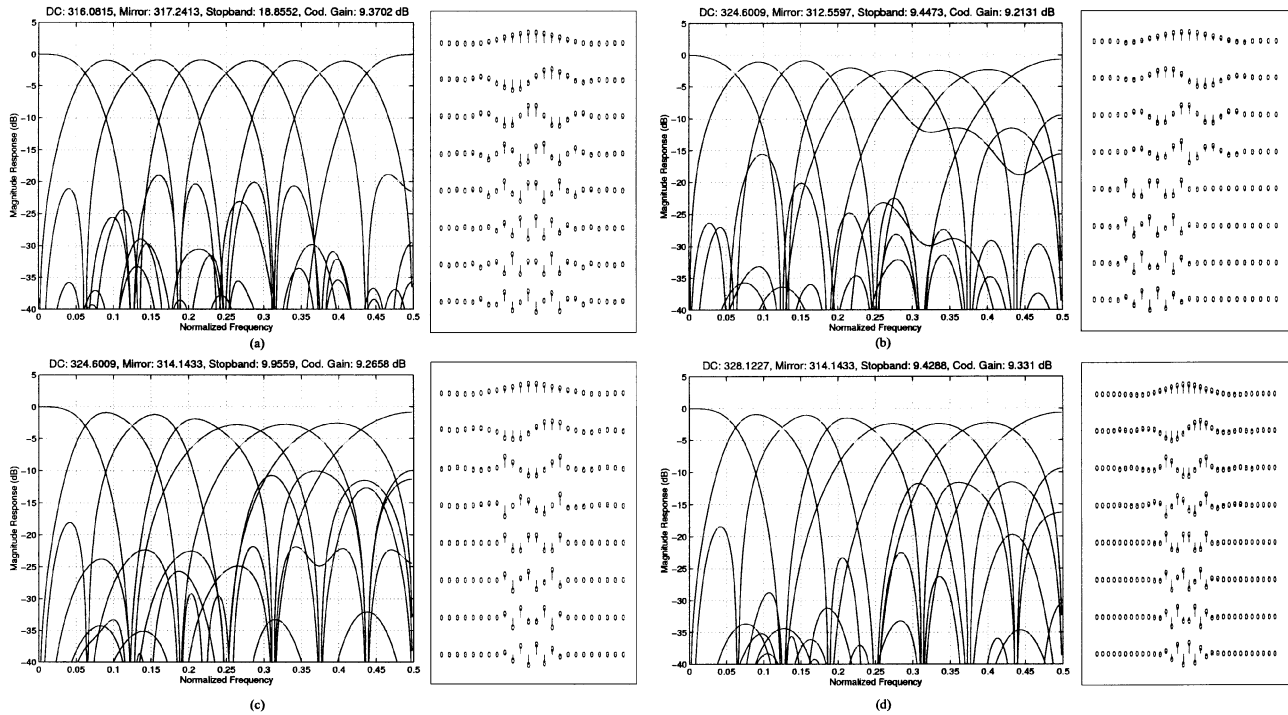


Fig. 7. Frequency and impulse responses of fast TFLOT examples. (a) 8×24 TFLOT (12 rotations, 9.37 dB). (b) 4×20 , 4×12 TFLOT (two rotations, 9.21 dB). (c) 4×24 , 4×8 TFLOT (three rotations, 9.27 dB). (d) 4×28 , 4×12 , 4×122 TFLOT (four rotations, 9.33 dB).

TABLE II
CODING RESULTS OF DIFFERENT TRANSFORMS (PSNR IN DECIBELS)

Comp. Ratio	SPIHT 9/7 WL	LOT-I	TFLOT			Comp. Ratio	SPIHT 9/7 WL	LOT-I	TFLOT		
			8×24	4×28 4×12	4×24 4×8				8×24	4×28 4×12	4×24 4×8
Barbara (512×512)						Boat (512×512)					
8 : 1	36.41	37.22	37.72	37.41	36.91	8 : 1	39.11	39.12	39.42	39.42	39.18
16 : 1	31.40	32.52	32.88	32.49	32.07	16 : 1	34.46	34.49	34.77	34.75	34.52
32 : 1	27.58	28.71	28.95	28.49	28.22	32 : 1	30.97	30.86	31.09	31.05	30.89
64 : 1	24.86	25.66	25.89	25.57	25.42	64 : 1	28.16	28.04	28.22	28.19	28.09
100 : 1	23.76	24.32	24.60	24.37	24.26	100 : 1	26.66	26.37	26.56	26.50	26.43
128 : 1	23.35	23.36	23.66	23.64	23.57	128 : 1	26.11	25.69	25.86	25.80	25.78
Lena (512×512)						Goldhill (512×512)					
8 : 1	40.41	40.02	40.30	40.30	40.12	8 : 1	36.55	36.56	36.69	36.65	36.50
16 : 1	37.21	36.69	37.08	37.02	36.77	16 : 1	33.13	33.12	33.28	33.21	33.08
32 : 1	34.11	33.49	33.90	33.80	33.57	32 : 1	30.56	30.52	30.68	30.62	30.55
64 : 1	31.10	30.43	30.79	30.69	30.55	64 : 1	28.48	28.34	28.50	28.47	28.44
100 : 1	29.35	28.59	28.94	28.89	28.81	100 : 1	27.38	27.08	27.26	27.25	27.21
128 : 1	28.38	27.60	27.99	27.95	27.89	128 : 1	26.73	26.46	26.64	26.63	26.60

C. Applications in Image Compression

In this section, we demonstrate the performance of various fast TFLOTs in image compression applications. The popular 9/7-tap biorthogonal wavelet and the LOT-I are used as benchmarks. The set partitioning in hierarchical trees (SPIHT) algorithm [21] is used to encode coefficients produced by all transforms.

The LOT-I and TFLOT transform coefficients are rearranged in analogy to the wavelet representation [17], [22], [23]. Further wavelet decomposition is employed to decorrelate the DC subband of the LOT-I/TFLOT coefficients. This ensures that the SPIHT coding algorithm has the same tree depth in all cases.

The objective coding results (PSNR in decibels) are tabulated in Table II for four popular 512×512 , eight-bit gray-scale test

images. Besides the wavelet transform and the LOT-I, three fast TFLOT examples in Fig. 7(a), (c), and (d) are evaluated.

It is well known that the images Lena and Barbara represent two extremes. The former is a very smooth image that is most suitable for wavelets, due to its long low-frequency basis function. On the other hand, the image Barbara has rich texture information, requiring fine high-frequency resolution to capture. As a result, lapped transforms can easily outperform wavelets.

Besides these special cases, Table II also reveals the following information:

- 1) The 8×24 TFLOT outperforms the wavelet transform in general. It also achieves an enhancement of more than 0.3 dB over the LOT-I in most cases, at the price of increased complexity.

- 2) The fast 4×28 , 4×12 TFLOT is superior to the LOT-I, except for three cases in Barbara. It can obtain an average improvement of 0.3 dB for Lena and Boat and 0.1 dB for Goldhill.
- 3) The performance of the fast 4×28 , 4×12 TFLOT is very similar to the 8×24 TFLOT. It also has better overall performance than the wavelet transform.
- 4) The fast 4×28 , 4×12 TFLOT consistently surpasses the 4×24 , 4×8 TFLOT (up to 0.5 dB), although only a minimal pre-processing unit is introduced.

Clearly, the 4×28 , 4×12 TFLOT provides a satisfactory tradeoff between the complexity and the performance, thanks to the fusion of pre- and post-processing of the DCT.

V. CONCLUSION

We present a general structure of LPPUFB with both pre- and post-processing modules added to the DCT. The proposed structure is more flexible than the existing DCT-based transforms like LOT, GenLOT, and the TDLT because LPPUFB with both partial-block overlapping and variable-length filters can be easily designed without having to modify the M -point DCT. A DCT-oriented initialization method is developed such that the optimization always starts from the DCT. It also helps to determine the sign parameters in modeling orthogonal matrices. Some high-performance and low-complexity DCT-based LP-PUFBs are developed, and their performance is demonstrated by image compression examples. The structure can be easily generalized to cover a large class of linear-phase perfect reconstruction filterbank by replacing each orthogonal matrix with an invertible matrix.

REFERENCES

- [1] K. R. Rao and P. Yip, *Discrete Cosine Transform: Algorithms, Advantages, Applications*. New York: Academic, 1990.
- [2] H. S. Malvar, *Signal Processing With Lapped Transforms*. Norwood, MA: Artech House, 1992.
- [3] H. S. Malvar and D. H. Staelin, "The LOT: Transform coding without blocking effects," *IEEE Trans. Signal Processing*, vol. 37, pp. 553–559, Apr. 1989.
- [4] R. L. de Queiroz, T. Q. Nguyen, and K. R. Rao, "The GenLOT: Generalized linear-phase lapped orthogonal transform," *IEEE Trans. Signal Processing*, vol. 44, pp. 497–507, Mar. 1996.
- [5] P. P. Vaidyanathan, *Multirate Systems and Filter Banks*. Englewood Cliffs, NJ: Prentice-Hall, 1993.
- [6] G. Strang and T. Q. Nguyen, *Wavelets and Filter Banks*. Wellesley, MA: Wellesley-Cambridge Press, 1997.
- [7] A. K. Soman, P. P. Vaidyanathan, and T. Q. Nguyen, "Linear phase paraunitary filter banks: Theory, factorizations and designs," *IEEE Trans. Signal Processing*, vol. 41, pp. 3480–3496, Dec. 1993.
- [8] T. D. Tran, R. L. de Queiroz, and T. Q. Nguyen, "Linear-phase perfect reconstruction filter bank: Lattice structure, design, and applications in image coding," *IEEE Trans. Signal Processing*, vol. 48, pp. 133–147, Jan. 2000.
- [9] X. Gao, T. Q. Nguyen, and G. Strang, "On factorization of M -channel paraunitary filterbanks," *IEEE Trans. Signal Processing*, vol. 49, pp. 1433–1446, July 2001.
- [10] L. Gan and K.-K. Ma, "A simplified lattice factorization for linear-phase perfect reconstruction filter bank," *IEEE Signal Processing Lett.*, vol. 8, pp. 207–209, July 2001.
- [11] X. Gao, Z. He, and X. G. Xia, "Efficient implementation of arbitrary-length cosine-modulated filter bank," *IEEE Trans. Signal Processing*, vol. 47, pp. 1188–1192, Apr. 1999.
- [12] R. D. Koilpillai and P. P. Vaidyanathan, "Cosine modulated FIR filter banks satisfying perfect reconstruction," *IEEE Trans. Signal Processing*, vol. 40, pp. 770–783, Apr. 1992.

- [13] T. Q. Nguyen and R. D. Koilpillai, "Theory and design of arbitrary-length cosine modulated filter banks and wavelets, satisfying perfect reconstruction," *IEEE Trans. Signal Processing*, vol. 44, pp. 473–486, Mar. 1996.
- [14] H. S. Malvar, "A pre- and post-filtering technique for the reduction of blocking effects," in *Proc. Picture Coding Symp.*, Stockholm, Sweden, June 1987.
- [15] T. D. Tran, J. Liang, and C. Tu, "Lapped transform via time-domain pre- and post-processing," *IEEE Trans. Signal Processing*, vol. 51, pp. XXXX–XXXX, June 2003.
- [16] T. D. Tran, R. de Queiroz, and T. Q. Nguyen, "Variable-length generalized lapped biorthogonal transform," in *Proc. IEEE Int. Conf. Image Process.*, vol. 3, Chicago, IL, Oct. 1998, pp. 697–701.
- [17] T. D. Tran, M. Ikehara, and T. Q. Nguyen, "Linear-phase paraunitary filter bank with filters of different lengths and its application in image compression," *IEEE Trans. Signal Processing*, vol. 47, pp. 2730–2744, Oct. 1999.
- [18] T. Nagai, M. Ikehara, M. Kaneko, and A. Kurematsu, "Generalized unequal length lapped orthogonal transform for subband image coding," *IEEE Trans. Signal Processing*, vol. 48, pp. 3365–3378, Dec. 2000.
- [19] J. Liang and T. D. Tran, "Further results on DCT-based linear phase paraunitary filter banks," in *Proc. IEEE Int. Conf. Image Processing*, vol. 2, Rochester, NY, Sept. 2002, pp. 681–684.
- [20] R. de Queiroz and K. R. Rao, "On reconstruction methods for processing finite-length signals with paraunitary filter banks," *IEEE Trans. Signal Processing*, vol. 43, pp. 2407–2710, Oct. 1995.
- [21] A. Said and W. A. Pearlman, "A new fast and efficient image codec based on set partitioning in hierarchical trees," *IEEE Trans. Circuits Syst. Video Technol.*, vol. 6, pp. 243–250, June 1996.
- [22] H. S. Malvar, "Fast progressive image coding without wavelets," in *Proc. Data Compression Conf.*, Mar. 2000, pp. 243–252.
- [23] Z. Xiong, O. G. Guleryuz, and M. T. Orchard, "A DCT-based embedded image coder," *IEEE Signal Processing Lett.*, vol. 3, pp. 289–290, Nov. 1996.



Jie Liang (S'99) received the B.E. and M.E. degrees from Xi'an Jiaotong University, Xi'an, China, in 1992 and 1995, respectively, and the M.E. degree from National University of Singapore (NUS) in 1998. He has been pursuing the Ph.D. degree at the Department of Electrical and Computer Engineering, the Johns Hopkins University, Baltimore, MD, since 1999.

He was with Hewlett-Packard Singapore and the Centre for Wireless Communications, NUS, from 1997 to 1999. His current research interests include multirate signal processing, image/video compressions, and digital communications.



Trac D. Tran (S'94–M'98) received the B.S. and M.S. degrees from the Massachusetts Institute of Technology, Cambridge, in 1993 and 1994, respectively, and the Ph.D. degree from the University of Wisconsin, Madison, in 1998, all in electrical engineering.

He joined the Department of Electrical and Computer Engineering, The Johns Hopkins University, Baltimore, MD, in July 1998, as an Assistant Professor. His research interests are in the field of digital signal processing, particularly in multirate systems, filterbanks, transforms, wavelets, and their applications in signal analysis, compression, processing, and communications.

Dr. Tran is an Associate Editor for the IEEE TRANSACTIONS ON SIGNAL PROCESSING as well as the IEEE TRANSACTIONS ON IMAGE PROCESSING. He was the co-director (with Prof. J. L. Prince) of the 33rd Annual Conference on Information Sciences and Systems (CISS'99), Baltimore, MD, in March 1999. He received the NSF CAREER Award in 2001. In the summer of 2002, he was an ASEE/ONR Summer Faculty Research Fellow at the Naval Air Warfare Center Weapons Division (NAWCWD), China Lake, CA.



Ricardo L. de Queiroz (SM'99) received the B.S. degree from Universidade de Brasilia, Brasilia, Brazil, in 1987, the M.S. degree from Universidade Estadual de Campinas, Campinas, Brazil, in 1990, and the Ph.D. degree from University of Texas at Arlington in 1994, all in electrical engineering.

From 1990 to 1991, he was with the DSP research group at Universidade de Brasilia as a research associate. He joined Xerox Corp., Webster, NY, in August 1994, where he is currently a member of the research staff at the IRIS Lab. He has published extensively in journals and conferences and contributed chapters to books as well. He also holds 25 issued patents, while many others are still pending. He is an Adjunct Faculty at the Rochester Institute of Technology, Rochester, NY. His research interests include multirate signal processing, image and signal compression, and color imaging.

Dr. de Queiroz received grants over all his graduate school years, including several scholarships and grants from the Brazilian government and awards and assistantships from universities. He is an Associate Editor for the IEEE SIGNAL PROCESSING LETTERS. He has been actively involved with the Rochester chapter of the IEEE Signal Processing Society, where he served as chair and organized the Western New York Image Processing Workshop since its inception. He is also part of the organizing committee of ICIP2002. He is a member of IS&T.